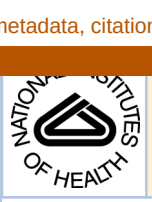

Published in final edited form as:

Organometallics. 2011 October 25; 30(22): 6233–6240. doi:10.1021/om200793p.

Enthalpy vs Entropy Driven Complexation of Homoallylic Alcohols by Rh(I) Complexes

Sung Ok Kang[†], **Vincent M. Lynch**[†], **Victor W. Day**[‡], and **Eric V. Anslyn**[†,*]

[†]Department of Chemistry and Biochemistry, The University of Texas at Austin, Austin, Texas 78712

[‡]Department of Chemistry, University of Kansas, Lawrence, Kansas 66045

Abstract

The thermodynamics of binding between several homoallylic alcohols and simple olefinic Rh(I) compounds was examined with ^{1}H NMR spectroscopy and ITC. ^{1}H NMR titrations revealed moderate binding of these alcohols with $[Rh(COD)_2]^+$ (**1**) and $[Rh(COD)(CH_3CN)_2]^+$ (**3**), but weaker binding with $[Rh(NBD)_2]^+$ (**2**). ITC indicated that the complexation with $[Rh(COD)_2]^+$ is mainly governed by enthalpy whereas binding with $[Rh(COD)(CH_3CN)_2]^+$ is entirely driven by entropy. The thermodynamic parameters for the homoallylic alcohol binding of Rh(I) complexes **1**–**3** are consistent with crystallographic data.

INTRODUCTION

Rh(I) complexes are used in a variety of different organometallic catalytic processes.[1,2] Several of these involve hydrogenative coupling reactions that use or generate homoallylic alcohols as reactants[3] or products,[4,5] respectively. Because many of these transformations have been reported with concomitant asymmetric induction, Rh(I) chemistry has been pursued for asymmetric synthesis.[6]

Inorganic coordination complexes, potentially those from Rh(I), could also be used to create optical signaling techniques for the high-throughput screening (HTS) of enantiometric excess (*ee*) values.[7,8] HTS methods[9] are becoming essential due to the rapid increase in the discovery of new asymmetric reactions using chiral catalysts created via parallel synthesis.[10] One logical approach to designing chiral inorganic complexes for enantioselective discrimination is to explore the actual chiral catalysts themselves.[11] We therefore decided to focus on chiral Rh(I) complexes for discriminating the enantiomers of homoallylic alcohols, but noticed a general lack of published thermodynamic data for the binding between Rh(I) with homoallylic alcohols,[3–5] even though calorimetry studies have been used by Hoff,[12] Marks,[13] Nolan,[14] and others[15] to determine the thermodynamic parameters for ligand coordination to other metals. The present work reports a series of studies aimed at uncovering the affinities between four Rh(I) species and several homoallylic (or analogous) alcohols, and determining their associated enthalpies and entropies of binding.

CORRESPONDING AUTHOR. anslyn@austin.utexas.edu. Telephone: 512-471-0068. Fax: 512-471-6835.
Sung Ok Kang is currently at Oak Ridge National Laboratory, Oak Ridge, TN 37830.

Supporting Information. ITC traces of the titration of $Rh(COD)_2$, $Rh(NBD)_2$, and $Rh(COD)(CH_3CN)_2$ into a $CHCl_3$ solution of **6**–**8**, a detailed description of the structure determination and refinement for **3**, ORTEP plots of **1** and **3**, selected bond lengths [Å] for **3**, and X-ray crystallographic data in CIF format for $Rh(COD)(CH_3CN)_2]BF_4$ (**3**). This material is available free of charge via the Internet at http://pubs.acs.org.

RESULTS AND DISCUSSION

The four Rh(I) complexes (**1**–**4**) studied were purchased from Aldrich and used without further purification. The binding studies of various alkenols (**5**–**10**) were first performed with $[Rh(COD)_2]OTf$ (**1**) using ^1H NMR titrations in $CDCl_3$ (Scheme 1). Fast exchange between bound and free homoallylic alcohols was seen on the NMR timescale (Figure 1). Upon addition of $[Rh(COD)_2]OTf$ into 4-penten-2-ol (**5**), H_b and H_c hydrogens were substantially shifted upfield ($\Delta\delta = -0.41$ and -1.26 ppm, respectively) while H_a and H_d were shifted downfield ($\Delta\delta = 0.10$ and 0.55 ppm, respectively). Alkene hydrogens of free COD, $[Rh(COD)_2]^+$, and $[Rh(COD)]^+$ appear at 5.57, 5.36, and 4.36 ppm, respectively (Figure 1a). Although two diastereomers can exist for the reaction of $[Rh(COD)_2]OTf$ (**1**) and racemic **5**, no appearance of two separate sets of signals are observed. This means either that one diastereomer predominates, or that they are exchanging faster than the NMR time scale. Similar trends of chemical shift changes were observed for other homoallylic alcohols (**6**–**8**), but to a lower extent. Binding constants were calculated from NMR titration curves using EQNMR,[16] and are listed in Table 1. The equilibrium constants were all of similar magnitude, ~500 M^{-1}.

Addition of allylic alcohol **9** to $[Rh(COD)_2]OTf$ (**1**), however, did not show any chemical shift changes (no binding). For 4-penten-1-ol (**10**), having an extended carbon chain, only slight chemical shift changes were observed, indicative of very weak binding (Figure 1b). Thus, the Rh(I) complex **1** is a selective receptor for homoallylic alcohols. The proposed binding modes of homoallylic alcohols with **1**–**4** are described in Scheme 1, where two coordination sites of rhodium occupied by COD, NBD, or $2CH_3CN$ are replaced by the homoallylic alcohol.[3a]

Addition of [Rh(*R*,*R*-DMPE)(COD)]BF_4 (**4**) to homoallylic alcohols showed no chemical shift changes indicating that the COD in this complex cannot be replaced by any of the alkenols. This is consistent with a sterically-induced displacement of the first COD ligand from **1**, and a higher affinity of Rh(I) for phosphines in **4**, and a high affinity of Rh(I) for a single COD ligand in **1**, **3** and **4**. Furthermore, the phosphines in **4** increase the binding affinity of COD relative to complexes **1** and **3**.

The binding between $[Rh(NBD)_2]OTf$ (**2**) and homoallylic alcohols resulted in similar chemical shift changes as with $[Rh(COD)_2]OTf$ (**1**), with the exception of the H_a hydrogen shifting slightly further upfield (Figure 1c). Alkene and bridgehead hydrogens are found at 6.75 and 3.58 ppm for free NBD, 5.03 and 4.02 ppm for $[Rh(NBD)_2]^+$, and 4.58 and 3.94 ppm for $[Rh(NBD)]^+$ (Figure 1c). Generally, **2** had lower alkenol affinities (Table 1) than **1** indicating that NBD is harder to replace than COD. We postulate that the considerably larger size and inherent flexibility of COD relative to that of NDB led to the increase in alkenol affinity for **1**.

Binding studies with $[Rh(COD)(CH_3CN)_2]BF_4$ (**3**) revealed similar chemical shift changes as with $[Rh(COD)_2]OTf$, but to a lower extend (Figure 1e). Although the same complex shown in Scheme 1 could be formed from **3** as with $[Rh(COD)_2]OTf$, the chemical shift changes of homoallylic alcohols were not identical when $[Rh(COD)_2]OTf$ (**1**) and $[Rh(COD)(CH_3CN)_2]BF_4$ (**3**) were added. We attributed this to the different counter anions, OTf^- and BF_4^- for **1** and **3**, respectively, and the expected tight ion-pairing in chlorofom. In fact, the chemical shift changes of **5** with $[Rh(COD)_2]BF_4$ were very similar to those with $[Rh(COD)(CH_3CN)_2]BF_4$ (**3**), although the peaks were broader (see Supporting Information). However, the binding constants of **3** for homoallylic alcohols were comparable or slightly larger than with **1**. We also examined the equilibrium constant (K_{eq})

in $CDCl_3$ for the binding of COD to $[Rh(COD)(CH_3CN)_2]BF_4$ (**3**) by integrating the ratio of free and bound COD upon addition of **3** to COD, revealing a value of 0.20 (Figure 2).

Job plot analyses[17] of **5** with **1** and **3** were used to determine the stoichiometry of the respective complexes. A total concentration of Rh(I) compound and **5** was maintained at 5 mM and the chemical shifts were recorded as a function of concentration ratios between zero and one. The plots showed a maximum value at 0.5 mole ratio, indicating a 1:1 stoichiometry (Figure 3).

Because the NMR studies revealed homoallylic alcohol binding to the Rh(I) compounds in chloroform, we moved to determining the driving force for complexation. Isothermal titration calorimetry (ITC)[18] was used to quantify the standard Gibbs-Helmholtz thermodynamic parameters ($\Delta H°$, $\Delta S°$, and $\Delta G°$).

The addition of 5μL aliquots of a solution of $[Rh(COD)_2]OTf$ (**1**) (10 mM) to a solution of **5** (1 mM) resulted in endothermic peaks in the ITC plots (Figure 4a). However, a reference experiment performed in the absence of **5** also showed endothermic heat changes (Figure 4d). Identical studies were performed with $[Rh(NBD)_2]OTf$ (**2**) and $[Rh(COD)(CH_3CN)_2]BF_4$ (**3**), yielding similar results (Figure 4). Nonlinear curve fitting was performed on the net heat changes (after substracting the reference data), revealing exothermic reactions with **1** and **2**, and endothermic reactions with **3** (Figure 5).

The curve fit of $[Rh(COD)_2]OTf$ using the ITC Origin software using a one binding site model converged on a 1:1 Rh compound:alkenol stoichiometry, and gave binding constants of 8.4×10^2, 7.8×10^2, 4.9×10^2, and 7.6×10^2 for **5**–**8**, respectively. Although these values are larger than those found via ^1H NMR, they are in reasonable agreement, given that they were determined by two completely different methods. The binding isotherm between $[Rh(COD)_2]OTf$ and **5** gave $\Delta H°$ and $T\Delta S°$ values of −4.4 and −0.40 kcal/mol, respectively. This result suggested that the homoallylic alcohol binding to $[Rh(COD)_2]OTf$ (**1**) was primarily driven by enthalpy. Similar enthalpy driven thermodynamics were observed with the other homoallylic alcohols (Table 1 and Figure 5a).

Analysis of the ITC with $[Rh(COD)(CH_3CN)_2]BF_4$ (**3**) is complicated by an inconsistent binding stoichiometry. The ITC software consistently converges on a 1 to 4~5 Rh complex-to-alkenol stoichiometry, even though Job plots show a 1:1 stoichiometry. And yet, the binding constants obtained from ITC were comparable to those from the NMR titrations. However, because of this inconsistency we caution placing confidence on the $\Delta H°$ and $\Delta S°$ values themselves, but instead we simply analyze the trends. The binding isotherm of **3** with **5** yielded a $\Delta H°$ value of 1.2 kcal/mol and a $T\Delta S$ value of 5.2 kcal/mol, indicating that binding with $[Rh(COD)(CH_3CN)_2]^+$ is nearly completely driven by entropy (Table 1, Figure 6). This favorable entropy change likely results from the release of two molecules of acetonitrile when only one molecule of **5** is bound. Similar thermodynamic parameters were seen with the other homoallylic alcohols **6**–**8** (Table 1 and Figure 5a).

The binding studies of alkenols to $[Rh(NBD)_2]OTf$ (**2**) revealed lower binding affinities with less favorable enthalpy, but more favorable entropy changes compared to **1** (Table 1 and Figure 5b). Hence, both enthalpic and entropic driving forces exist for binding to this complex. One might expect that the release of the more conformationally flexible COD ligand from **1** would be more entropically favored than release of NBD from **2**, but we find the opposite. A possible explanation is that $\Delta S°$ for the reaction with **1** is balanced by another effect. The two bulky COD ligands in **1** are buttressed up against each other, as seen in the crystal structure of **1**, and have very close H···H contacts ranging from 1.76 to 1.91 Å (average = 1.84 Å). These are considerably shorter than the 2.18 Å van der Waals diameter[19] of hydrogen (Figure 7a and b).[20] These short intraligand H···H contacts lengthen

(weaken) the ethylenic Rh–C bonds in $[Rh(COD)_2]OTf$ (**1**) (ranging from 2.20 to 2.27 Å; average = 2.24 Å) relative to the corresponding ethylenic Rh–C bonds in $[Rh(COD)(CH_3CN)_2]BF_4$ (**3**) (ranging from 2.04 to 2.21 Å; average = 2.14 Å) which is not sterically-crowded (Figure 7e and f). The average ethylenic Rh–C bond for **1** is 0.10 Å longer than that for **3**. The weaker Rh-C bonds produced by these unfavorably close contacts in **1** can lead to increased ligand motion. This could result in a smaller entropy increase than expected for releasing the COD and binding the alkenol. Dissociation of a COD ligand from **1** would allow the remaining COD to bind more strongly to the Rh, enhancing $\Delta H°$ for the reaction and giving a small overall $\Delta S°$ (Table 1). $[Rh(COD)(CH_3CN)_2]BF_4$ (**3**), with a strongly bound COD, revealed a similar $\Delta G°$ to **1** upon alkenol binding with slightly unfavorable enthalpic changes that are compensated by more favorable entropic gain.

The more compact nature of NBD compared to COD eliminates the severely short interligand H···H in **2** (Figure 7c and d). The **e**thylenic H···H contacts in $[Rh(NBD)_2]SbF_6$ range from 2.54 to 2.57 Å compared to the 1.76 to 1.91 Å in **1**.[21] The Rh–C distances in $[Rh(NBD)_2]^+$ range from 2.20 to 2.21 Å (average = 2.205 Å). Since the NBD ligands in **2** are more strongly bound to Rh than the COD ligands in **1**, replacement of the second NBD by alkenol could give a larger $\Delta S°$ than for the corresponding reaction with **1**. This hypothesis is supported by the crystal structures of **1** – **3**, and it explains the thermodynamic behavior of the complexation of Rh compounds and homoallylic alcohols.

Our study showing that ligand binding in similar complexes can switch between enthalpy and entropy driving forces has previous precedent. For bisphosphonate complexes of the FPPS enzyme, the binding of bisphosphonates with neutral side chains is enthalpy-driven whereas bisphosphonates with charged side chains bind in an entropy-driven manner.[22] The lanthanide complexes of neutral tripodal ligands also showed different driving forces where the formation of the complexes of tetradentate versus heptadentate ligands was enthalpy and entropy-driven, respectively.[23]

SUMMARY

In summary, thermodynamic studies of homoallylic alcohol complexation with Rh complexes (**1**–**3**) was carried out using ^1H NMR and ITC experiments. Upon binding significant chemical shift changes of the homoallylic alcohol hydrogens were observed in NMR spectroscopy. ITC experiments revealed that the binding of homoallylic alcohols with $[Rh(COD)_2]OTf$ (**1**) is mainly driven by enthalpy while binding to $[Rh(COD)(CH_3CN)_2]BF_4$ (**3**) is governed by entropy. However the binding of alkenols to $[Rh(NBD)_2]OTf$ (**2**) was accompanied by both favorable enthapy and entropy changes. These thermodynamic data are consistent with the crystal structures of Rh complexes (**1**–**3**). This investigation furthers our basic understanding of the thermodynamics for complexation in organometallic complexes.

EXPERIMENTAL SECTION

General Considerations

The chemicals used were obtained from Aldrich and were used without further purification, except where noted. ^1H NMR spectra were recorded on a Varian Mercury spectrometer at 300MHz or 400 MHz. The titration apparatus for the ITC experiments was purchased from Microcal Inc. The VP-ITC instrument is interfaced with Origin (version 5) software for both data collection and data analysis. Chloroform was purified using basic alumina column chromatography to remove all the residual HCl.

NMR titration

Each titration was performed by 7 measurements in $CDCl_3$ at room temperature. Aliquots from a stock solution of the Rh complex (250 mM) were gradually added to the initial solution of analyte, homoallylic alcohol (5 mM). All proton signals were referred to a TMS standard. The association constants *K* were calculated by EQNMR.[16]

Job plot

Job plots were performed from ^{1}H NMR measurements of Rh compound and homoallylic alcohol with different concentration ratios in solvent $CDCl_3$. The total concentrations of Rh compound and alkenol solution were maintained as 5 mM. All ^{1}H NMR spectra were recorded at room temperature. The stoichiometric ratio of Rh compound to alkenol in complex was obtained by plotting of [**Rh**]/([**Rh**] + [**A**]) against Δδ([**A**]/([**Rh**] + [**A**]), where Δδ is the chemical shift change of H_b protons of alkenol.[17]

ITC experiments

The reference cell was filled with chloroform and the titration cell was filled with chloroform solution of homoallylic alcohol (1 mM). For the control experiment, both reference and titration cells were filled with chloroform. The syringe was filled with approximately 300 μL of a solution of $[Rh(COD)(CH_3CN)_2]BF_4$ (10 mM). The syringe was fitted above the cell and the following parameters set: Injection size = 5 μL, Number of injections = 60, Temperature = 23 °C, Injection Interval = 180 sec, Cell Feedback = 20 μcal. The Origin software was used to apply a 1:1 binding algorithm to the data, the fit of which yields a binding affinity, enthalpy change, and binding stoichiometry for the titration.

X-ray experimental

Crystals of **3** suitable for X-ray diffraction structural studies were obtained by the slow evaporation of a saturated $MeOH/CH_3CN/CH_3CO_2C_2H_5$ solution of $[Rh(COD)(CH_3CN)_2]BF_4$. Single-crystal X-ray diffraction data for $[Rh(COD)(CH_3CN)_2]BF_4$ (**3**) were collected on a Bruker APEX II diffractometer equipped with Helios multilayer x-ray optics. X-rays were provided by a Bruker MicroStar microfocus Cu rotating anode (λ = 1.54178 Å) generator operating at 45 kV and 60 mA. The structure was solved by direct methods and refined on F^2 using the SHELXTL software package. Absorption corrections were applied using SADABS, part of the SHELXTL package. Crystal data and refinement parameters are summarized in Table 2. A detailed description of the structure determination and refinement is given in the Supporting Information.

Supplementary Material

Refer to Web version on PubMed Central for supplementary material.

Acknowledgments

The authors thank the National Institutes of Health, NIH-R01GM065515, and the Welch Foundation, F-1151, for support of this work as well as the National Science Foundation, CHE-0923449, for the purchase of the x-ray diffractometer used to collect diffraction data for **3**.

REFERENCES

1. (a) Evans, PA., editor. Modern Rhodium-Catalyzed Organic Reactions. Weinheim: Wiley-VCH; 2005. (b) Tarui A, Sato K, Omote M, Kumadaki I, Ando A. Adv. Synth. Catal. 2010; 352:2733–2744.(c) Gual A, Godard C, Castillon S, Carmen C. Tetrahedron: Asymmetry. 2010; 21:1135–1146. (d) Edwards HJ, Hargrave JD, Penrose SD, Frost CG. Chem. Soc. Rev. 2010; 39:2093–2105.

[PubMed: 20407730] (e) Minnaard AJ, Feringa BL, Lefort L, de Vries JG. Acc. Chem. Res. 2007; 40:1267–1277. [PubMed: 17705446]

2. (a) Krische, MJ., editor. Topics in Current Chemistry. Vol. Vol. 279. Berlin, Heidelberg: Springer-Verlag; 2007. (b) Tamaru, Y., editor. Modern Organonickel Chemistry. Weinheim: Wiley-VCH; 2005.
3. (a) Zhao P, Incarvito CD, Hartwig JF. J. Am. Chem. Soc. 2006; 128:9642–9643. [PubMed: 16866513] (b) Sumida Y, Takada Y, Hayashi S, Hirano K, Yorimitsu H, Oshima K. Chem. Asian J. 2008; 3:119–125. [PubMed: 18034441] (c) Ahisten N, Martin-Matute B. Adv. Synth. Catal. 2009; 351:2657–2666.(d) Rosenberg S, Leino R. Tetrahedron Lett. 2009; 50:5305–5307.(e) Shintani R, Takatsu K, Hayashi T. Org. Lett. 2008; 10:1191–1193. [PubMed: 18303902] (f) Jang M, Hayashi S, Hirano K, Yrimitsu H, Oshima K. Tetrahedron Lett. 2007; 48:4003–4005.(g) Takada Y, Hayashi S, Hirano K, Yrimitsu H, Oshima K. Org. Lett. 2006; 8:2515–2517 4. [PubMed: 16737302]
4. (a) Han SB, Kim IS, Krische MJ. Chem. Commun. 2009:7278–7287.(b) Bower JF, Kim IS, Patman RL, Krische MJ. Angew. Chem. Int. Ed. 2009; 48:34–46.(c) Ngai M–Y, Kong J–R, Krische MJ. J. Org. Chem. 2007; 72:1063–1072. [PubMed: 17288361] (d) Jang H–Y, Krische MJ. Acc. Chem. Res. 2004; 37:653–661. [PubMed: 15379581]
5. (a) Tamaru Y, Kimura M. Org. Synth. 2006; 83:88–96.(b) Kimura M, Nojiri D, Fukushima M, Oi S, Sonoda Y, Inoue Y. Org. Lett. 2009; 11:3794–3797. [PubMed: 19663391] (c) Bing Y, Menard F, Isono N, Lautens M. Synthesis. 2009:853–859.(d) Vasylyev M, Alper H. J. Org. Chem. 2010; 75:2710–2713. [PubMed: 20232839]
6. (a) Christmann, M.; Braese, S., editors. Asymmetric Synthesis-The Essentials. Weinheim, Germany: Wiley-VCH; 2007. (b) Lin, G–Q.; Li, Y–M.; Chan, ASC. Principles and Applications of Asymmetric Synthesis. New York: Wiley; 2001.
7. (a) Leung D, Folmer-Andersen JF, Lynch VM, Anslyn EV. J. Am. Chem. Soc. 2008; 130:12318–12327. [PubMed: 18714996] (b) Leung D, Anslyn EV. J. Am. Chem. Soc. 2008; 130:12328–12333. [PubMed: 18714993] (c) Folmer-Andersen JF, Kitamura M, Anslyn EV. J. Am. Chem. Soc. 2006; 128:5652–5653. [PubMed: 16637629] (d) Zhu L, Shabbir SH, Anslyn EV. Chem. Eur. J. 2006; 13:99–104. [PubMed: 17066491] (e) Shabbir SH, Regan CJ, Anslyn EV. Proc. Natl. Acad. Sci. 2009; 106:10487–10492. [PubMed: 19332790] (f) Nieto S, Lynch VM, Anslyn EV, Kim H, Chin J. J. Am. Chem. Soc. 2008; 130:9232–9233. [PubMed: 18572934]
8. (a) Mei X, Wolf C. J. Am. Chem. Soc. 2006; 128:13326–13327. [PubMed: 17031923] (b) Liu S, Pestano JPC, Wolf C. J. Org. Chem. 2008; 73:4267–4270. [PubMed: 18454551] (c) Holmes AE, Zahn S, Canary JW. Chirality. 2002; 14:471–477. [PubMed: 12112340] (d) Zhang J, Holmes AE, Sharma A, Brooks NR, Rarig RS, Zubieta J, Canary JW. Chirality. 2003; 15:180–189. [PubMed: 12520510] (e) Corradini R, Paganuzzi C, Marchelli R, Pagliari S, Sforza S, Dossena A, Galaverna G, Duchateau A. J. Mater. Chem. 2005; 15:2741–2746.(f) Corradini R, Paganuzzi C, Marchelli R, Pagliari S, Dossena A, Duchateau A. J Inclusion Phenom. Macrocyclic Chem. 2007; 57:625–630.
9. (a) Tsukamoto M, Kagan HB. Adv. Synth. Catal. 2002; 344:453–463.(b) Finn MG. Chirality. 2002; 14:534–540. [PubMed: 12112324] (c) Pu L. Chem. Rev. 2004; 104:1687–1716. [PubMed: 15008630] (d) Charbonneau V, Ogilvie WW. Mini-Rev. Org. Chem. 2005; 2:313–332.
10. (a) Reetz MT. Angew. Chem. Int. Ed. 2001; 40:284–310.(b) Loch JA, Crabtree RH. Pure Appl. Chem. 2001; 73:119–128.(c) Shimizu KD, Snapper ML, Hoveyda AH. Chem. Eur. J. 1998; 4:1885–1889.(d) Sprout CM, Richmond ML, Seto CT. J. Org. Chem. 2005; 70:7408–7417. [PubMed: 16122266]
11. He X, Zhang Q, Wang W, Lin L, Liu X, Feng X. Org. Lett. 2011; 13:804–807. [PubMed: 21247141]
12. (a) Germain ME, Temprado M, Castonguay A, Kryatova OP, Rybak-Akimova EV, Curley JJ, Mendiratta A, Tsai Y–C, Cummins CC, Prabhakar R, McDonough JE, Hoff CD. J. Am. Chem. Soc. 2009; 131:15412–15423. [PubMed: 19919164] (b) Achord P, Fujita E, Muckerman JT, Scott B, Fortman GC, Temprado M, Cai X, Captain B, Isrow D, Weir JJ, McDonough JE, Hoff CD. Inorg. Chem. 2009; 48:7891–7904. [PubMed: 19621935] (c) Fortman GC, Captain B, Hoff CD. Inorg. Chem. 2009; 48:1808–1810. [PubMed: 19235943]
13. (a) Sonnenberger DC, Morss LR, Marks TJ. Organometallics. 1985; 4:352–355.(b) Schock LE, Marks TJ. J. Am. Chem. Soc. 1988; 110:7701–7715.(c) Nolan SP, Stern D, Marks TJ. J. Am.

Chem. Soc. 1989; 111:7844–7853.(d) Deck PA, Marks TJ. J. Am. Chem. Soc. 1995; 117:6128–6129.

14. (a) Smith DC Jr, Stevens ED, Nolan SP. Inorg. Chem. 1999; 38:5277–5281.(b) (a) Wang K, Goldman AS, Li C, Nolan SP. Organometallics. 1995; 14:4010–4013.(c) Maar CM, Huang J, Nolan SP. Organometallics. 1998; 17:5018–5024.(d) Huang J, Haar CM, Nolan SP, Marshall WJ, Moloy KG. J. Am. Chem. Soc. 1998; 120:7806–7815.(e) Serron S, Nolan SP. Organometallics. 1996; 15:4301–4306.
15. (a) Blackmond DG. Angew. Chem. Int. Ed. 2005; 44:4302–4320.(b) Burke NE, Singhal A, Hintz MJ, Ley JA, Hui H, Smith LR, Blake DM. J. Am. Chem. Soc. 1979; 101:74–79.(c) Jesse AC, Cordfunke EHP, Ouweltjes W. Thermochim. Acta. 1979; 30:293–302.
16. Hynes MJ. J. Chem. Soc. Dalton Trans. 1993:311–312.
17. (a) Job P. Ann. Chim. 1928; 9:113–203.(b) Blanda MT, Horner JH, Newcomb M. J. Org. Chem. 1989; 54:4626–4636.
18. Stodeman M, Wadso I. Pure Appl. Chem. 1995; 67:1059–1068.(b) Wadso I. Trends Biotechnol. 1986; 4:45–51.(c) Wiseman T, Williston S, Brandts JF, Lin LN. Anal. Biochem. 1989; 179:131–137. [PubMed: 2757186]
19. (a) Bondi A. J. Phys. Chem. 1964; 68:441–452.(b) Rowland RS, Taylor R. J. Phys. Chem. 1996; 100:7384–7391.
20. (a) Baenziger NC, Mottel EA, Doyle JR. Acta Crystallogr. Sect. C: Cryst. Struct. Commun. 1991; C47:539–541.(b) Dahlenburg L, Osthoff N, Heinemann FW. Acta Crystallogr. Sect. E: Struct. Rep. 2001; E57:m117–m118.
21. Kölle U, Görissen R, Wagner T. Chem. Ber. 1995; 128:911–917.
22. Yin F, Cao R, Goddard A, Zhang Y, Oldfield E. J. Am. Chem. Soc. 2006; 128:3524–3525. [PubMed: 16536518]
23. Bravard F, Rosset C, Delangle P. Dalton Trans. 2004:2012–2018. [PubMed: 15252589]

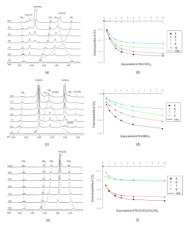

Figure 1.
^{1}H NMR titration of (a) **1**, (c) **2**, and (e) **3** into **5** (numbers at the left side indicate the equivalents of Rh complexes added), and binding curves of (b) **1**, (d) **2**, and (f) **3** for **5**–**8**. All in $CDCl_3$.

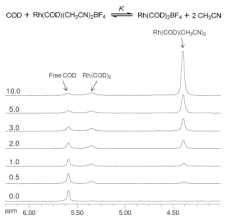

Figure 2.

^{1}H NMR titration between cyclooctadiene (COD) and [Rh(COD)($CH_3CN)_2$]BF_4 (**3**) (numbers at the left side indicate the equivalents of **3** added).

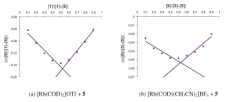

Figure 3.
Job plot of **5** with (a) $[Rh(COD)_2]OTf$ and (b) $[Rh(COD)(CH_3CN)_2]BF_4$ in $CHCl_3$ at room temperature. Total concentration of [**5** + **1**] = 5 mM and [**5** + **3**] = 5 mM.

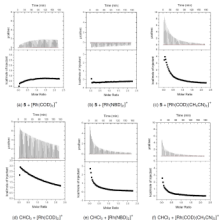

Figure 4.
ITC traces of the titration of $[Rh(COD)_2]OTf$ (a and d), $[Rh(NBD)_2]OTf$ (b and e), and $[Rh(COD)(CH_3CN)_2]BF_4$ (c and f) into a $CHCl_3$ solution of **5** (1 mM) and blank (reference) at 296 K.

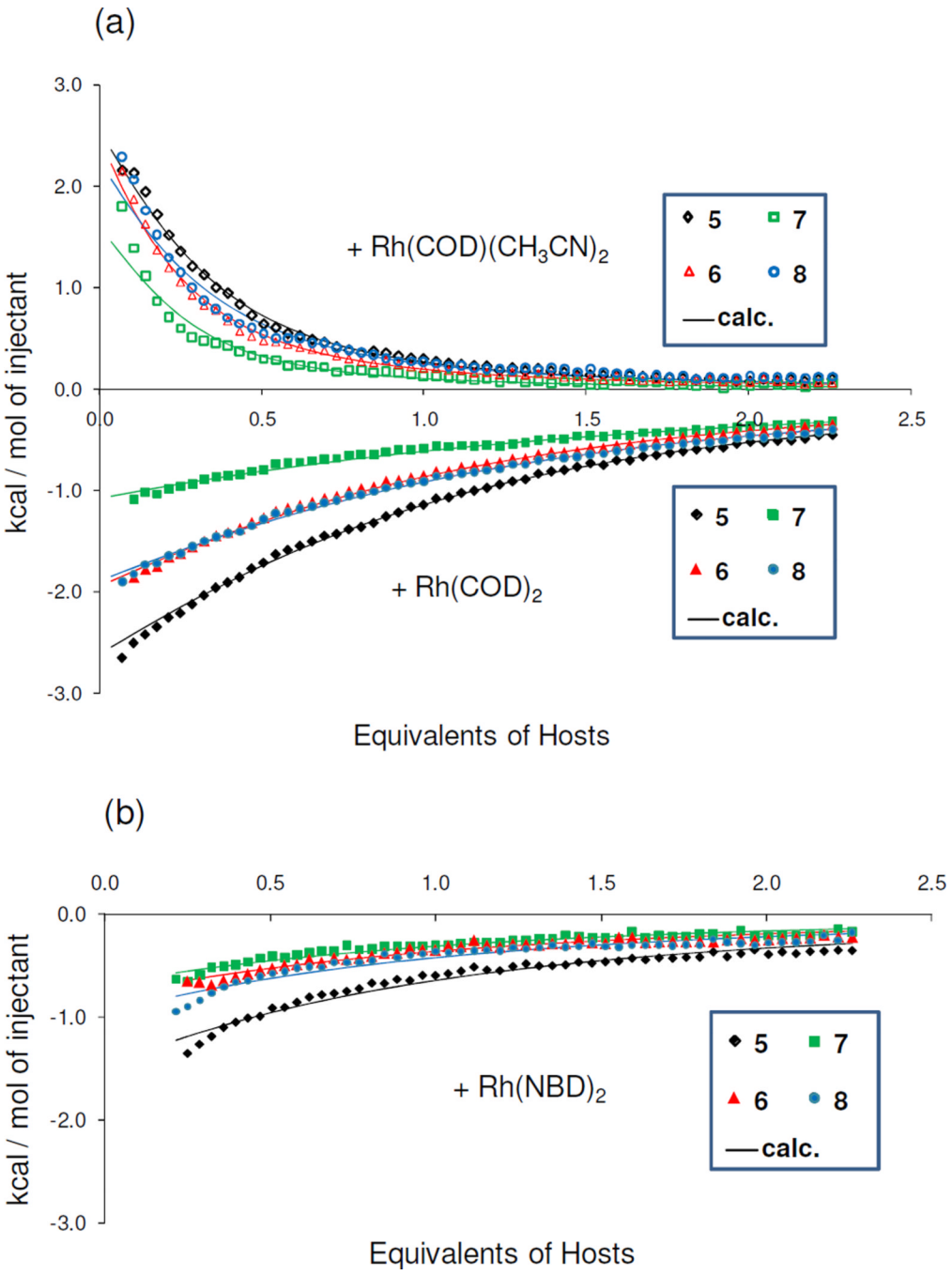

Figure 5.

Binding isotherms of the complexes of **5**–**8** to (a) $[Rh(COD)_2]OTf$ (solid markers) and $[Rh(COD)(CH_3CN)_2]BF_4$ (open markers), and (b) $[Rh(NBD)_2]OTf$ in $CHCl_3$ at 296 K. The solid lines represent the best fit.

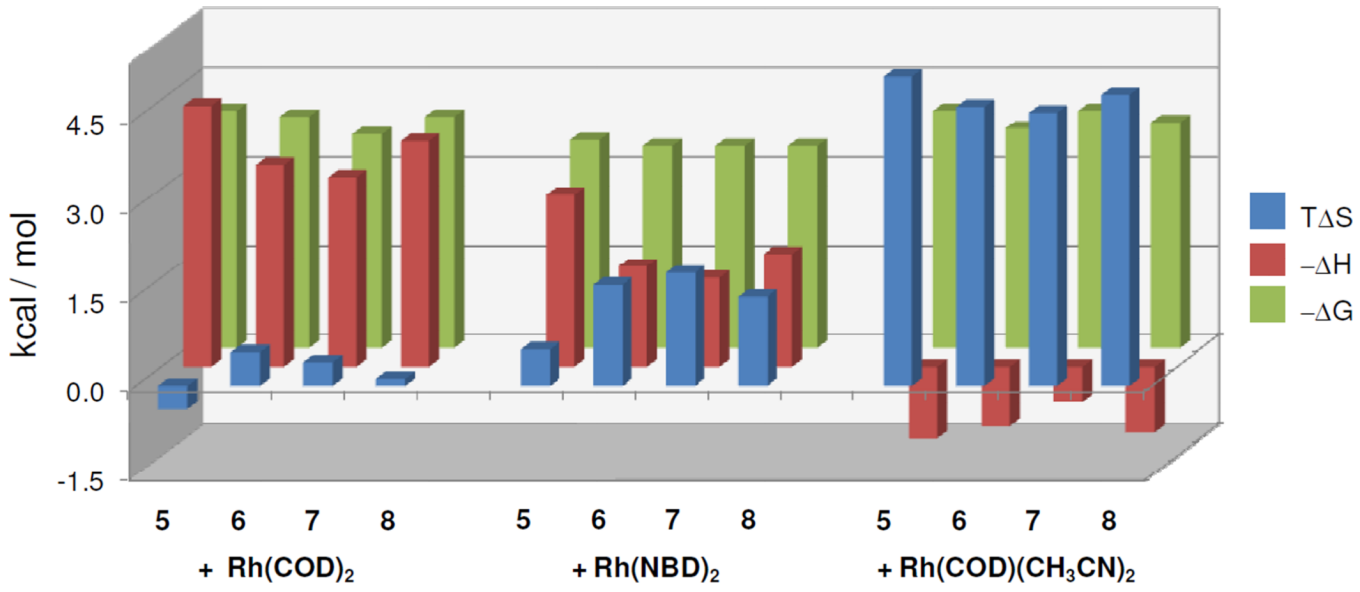

Figure 6.
Comparison of the binding energetics of the complexes of **5**–**8** with **1**, **2**, and **3** in $CHCl_3$.

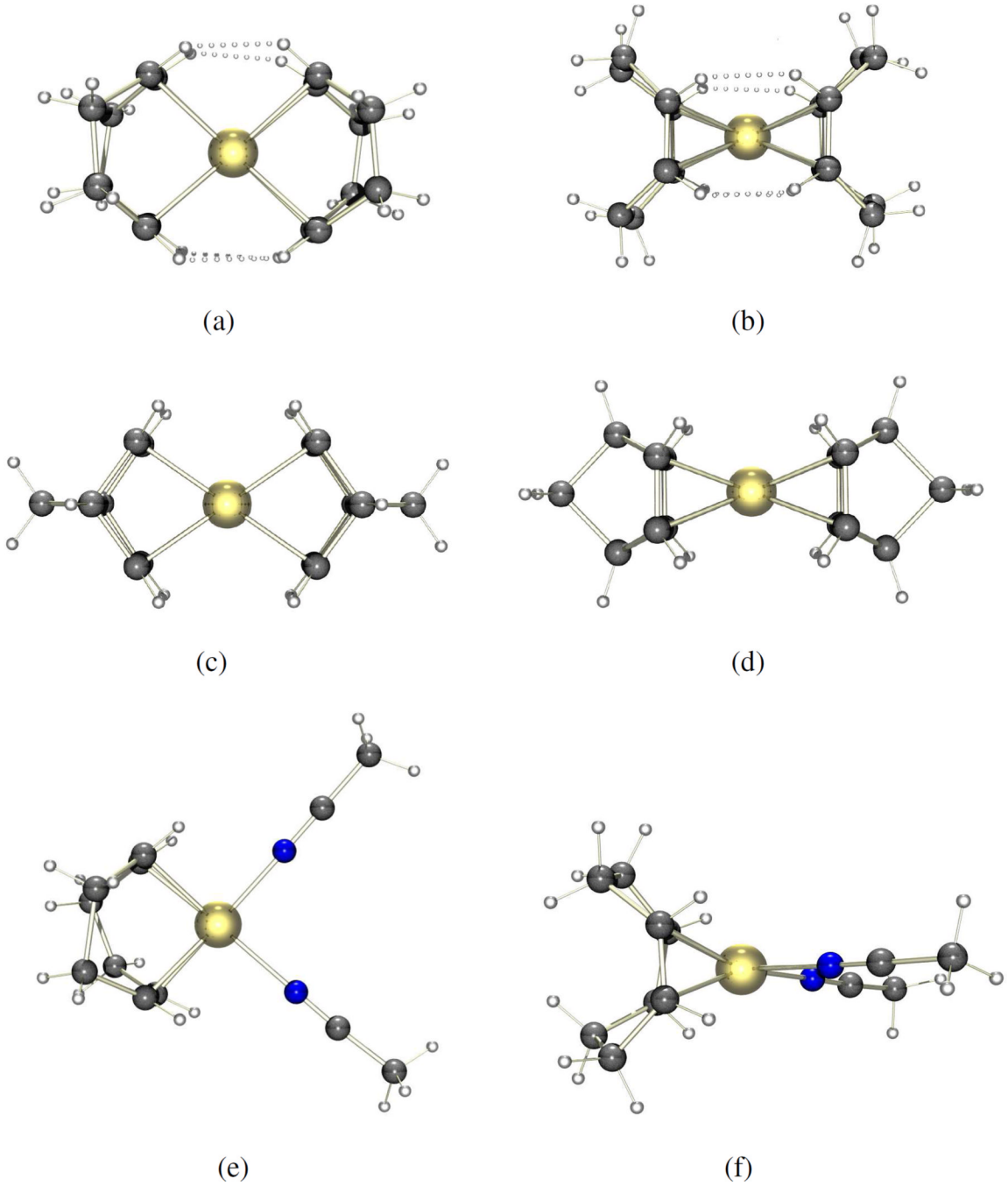

Figure 7.
Top and side views of crystal structures of $[Rh(COD)_2]OTf$ (a and b),[20] $[Rh(NBD)_2]SbF_6$ (c and d),[21] and $[Rh(COD)(CH_3CN)_2]BF_4$ (e and f). Short intraligand H···H contacts are shown with dotted lines in **1**. The counter anions are omitted for clarity.

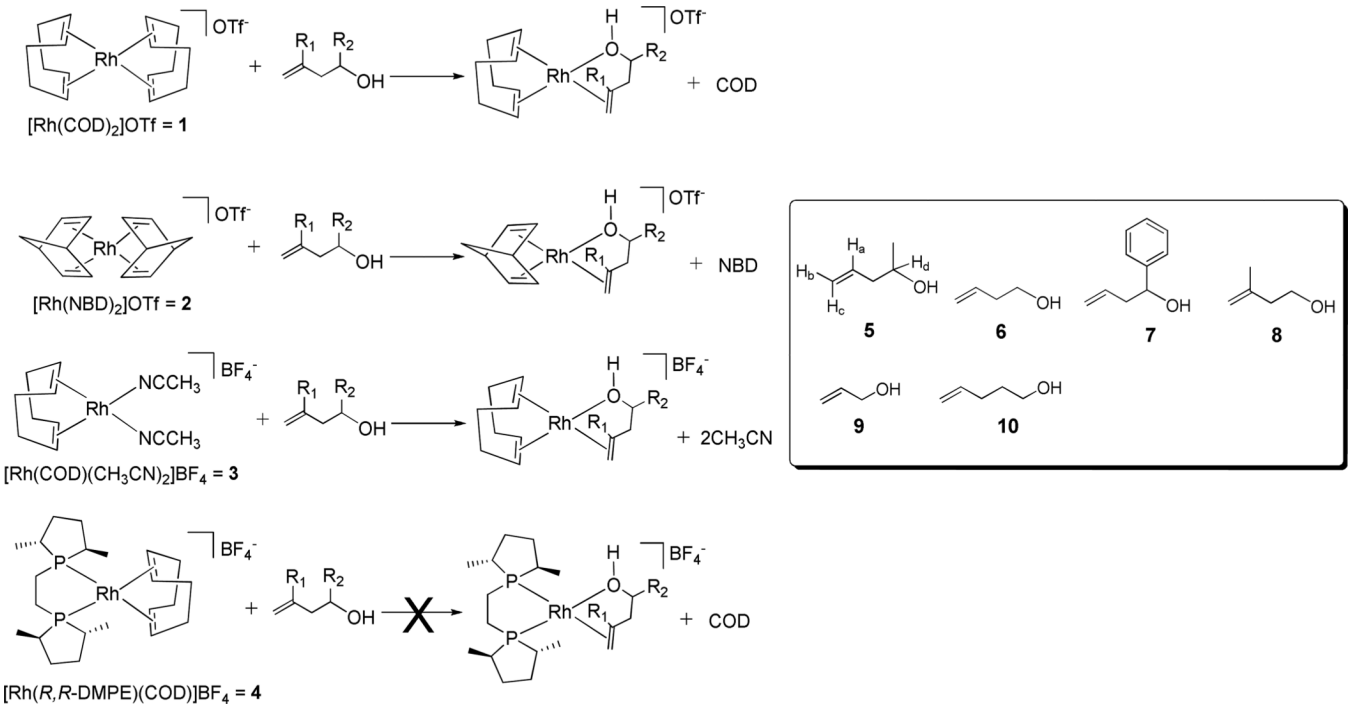

Scheme 1.

Proposed binding mode of homoallylic alcohols with Rh(I) complexes

COD = Cyclooctadiene, NBD = Norbornadiene, DMPE = Dimethylphospholanoethane, Tf = Triflate

Table 1

Association constants and thermodynamic parameters for the binding of Rh(I) complexes (**1–3**) and homoallylic alcohols (**5–8**).[a]

Rh(I) complex	Homoallylic alcohol	K^a (M^{-1})	$\Delta H°$ (kcal/mol)	$T\Delta S°$ (kcal/mol)	$\Delta G°$ (kcal/mol)
1	**5**	540 (840)	−4.4	−0.40	−4.0
	6	400 (780)	−3.4	0.56	−3.9
	7	560 (490)	−3.2	0.39	−3.6
	8	570 (760)	−3.8	0.12	−3.9
2	**5**	150 (360)	−2.9	0.61	−3.5
	6	75 (310)	−1.7	1.7	−3.4
	7	41 (320)	−1.5	1.9	−3.4
	8	79 (340)	−1.9	1.5	−3.4
3	**5**	520 (860)	1.2	5.2	−4.0
	6	700 (530)	1.0	4.7	−3.7
	7	980 (990)	0.58	4.6	−4.0
	8	890 (660)	1.1	4.9	−3.8

[a] Binding constants were determined by ^{1}H NMR titrations in $CDCl_3$ at room temperature. Binding constants in parenthesis and thermodynamic parameters are determined by ITC titrations in $CHCl_3$ at 296 K. Errors ≤10%.

Table 2

Crystal data and structure refinement for $[Rh(COD)(CH_3CN)_2]BF_4$ (**3**).

	$[Rh(COD)(CH_3CN)_2]BF_4$
Empirical formula	$C_{12}H_{18}BF_4N_2Rh$
Fw	380.00
cryst syst	Monoclinic
space group	$P2_1/c$
a (Å)	10.3051(5)
b (Å)	20.6989(9)
c (Å)	34.951(2)
α (deg)	90
β (deg)	98.466(2)
γ (deg)	90
V (Å^3)	7374.0(6)
Z	20
diffractometer	Bruker APEX II; Cu rotating anode
d_{calcd} (Mg/m^3)	1.711
λ (Å)	1.54178
T (K)	100(2)
F(000)	3800
abs coeff(mm^{-1})	9.702
Abs corr	Multi-scan
Max, min transm	0.7532, 0.5630
frame time (s)	2–8 sec
lattice constants: # peak centers	9642
θ range (deg)	1.28–69.12
Reflns collected	81657
independent reflections/R_{int}	12944/0.0422
% completeness	93.2
data/restraints/ params	12944/570/902
data observed (I>2σ)	5680

	[Rh(COD)(CH$_3$CN)$_2$]BF$_4$
R_1(obsd); wR_2(all)[a]	0.0490; 0.1364
GOF (F^2)	1.075

[a] $R_1 = \Sigma \| F_0| - |F_0| \| / \Sigma | F_0|$. $wR_2 = \{\Sigma [w(F_0^2 - F_c^2)^2] / \Sigma [w(F_0^2)^2]\}^{1/2}$